

Metal-insulator transition in highly conducting oriented polymers

N. Dupuis*

Department of Physics, University of Maryland, College Park, Maryland 20742-4111

(Received 3 December 1996)

We suggest that highly conducting oriented polymers with a fibril structure can be modeled by a regular lattice of disordered metallic wires with a random first-neighbor interwire coupling which mimics the cross links between fibrils. We determine the position of the metal-insulator transition (MIT) as a function of interwire cross-link concentration, interwire coupling J , and number M of polymer chains in a wire. Two different approaches are used. The first one is based on the self-consistent diagrammatic theory of Anderson localization. In the second approach, we show that the MIT can be described by a nonlinear σ model. For $M = 1$, we find that a small value of J favors the metallic state while a large value of J induces localization in agreement with recent numerical calculations. When $M \gg 1$, an increase of J always favors a delocalization of the electronic states in agreement with a previous analytical analysis. [S0163-1829(97)08630-X]

I. INTRODUCTION

Highly conducting doped polymers based on polyacetylene, polypyrrole, and polyaniline have recently attracted considerable interest. Due to the advent of improved chemical processing, their room-temperature conductivity can be comparable to that of copper. A T -independent Pauli susceptibility, a linear T dependence of thermoelectric power, and a large negative microwave dielectric constant further suggest that highly conducting polymers are intrinsically metallic. However, in contrast to traditional metals, their conductivity decreases with temperature. This latter property is usually explained by the fact that highly conducting polymers are close to a metal-insulator transition driven by disorder.¹ The decrease of the conductivity with T then results from phonon-controlled localization effects. Motivated by these experimental results, many explanations of the transport properties of highly conducting polymers are based on dirty quasi-one-dimensional conductors (i.e., weakly coupled chains systems).² The assumption of a periodic arrangement of the one-dimensional (1D) polymers chains which underlies such explanations is however quite unrealistic. Prigodin and Efetov (PE) have recently proposed a model which takes into account the irregular structure of the polymers.³ In highly conducting polymers, single chains are coupled into fibrils which are bent in space in a very complicated way. PE model the fibrils by weakly disordered metallic wires. The cross links between the fibrils are described by interwire junctions. In the absence of junctions, all electronic states of the wires are localized by any weak disorder. PE have shown that the interwire junctions lead to a MIT and determined the position of the transition and the critical behavior.

We suggest in this paper that highly conducting oriented polymers with a fibril structure can be modeled by a regular lattice of disordered metallic wires with a random first-neighbor interwire coupling. (In *oriented* polymers, the fibrils, although randomly bent in space, follow on average the direction of highest conductivity.) The case where the wires contain a single chain has been recently studied numerically by Zambetaki, Economou, and Evangelou (ZEE).⁴ We use two different approaches to study the MIT in this

system. The first one is based on the self-consistent diagrammatic theory (SCDT) introduced by Vollhardt and Wölfle.⁵ In the second approach, we show that the MIT can be described by a nonlinear σ model (NL σ M). Both approaches yield the same phase diagram. For a large number M of 1D chains in the fibrils, we recover the main result of PE: an increase of the interwire coupling J favors a delocalization of the electronic states. However, we obtain a different critical behavior and the position of the transition differs from the result of PE. When $M = 1$, we show that a small value of J favors the metallic state while a large value of J induces localization in agreement with the numerical calculation of ZEE.

II. THE MODEL

We consider PE's model in the case of strongly oriented polymers and make the following Gedanken experiment: we stretch the wires in such a way that they form a regular (square) lattice of straight and parallel wires (Fig. 1). The interwire junctions now correspond to couplings between neighboring wires. In the case of a strongly oriented polymer, these couplings will have a short range. It is then possible, without inducing any qualitative change, to consider a simpler model where the couplings are allowed only between first-neighbor wires and in a direction which is perpendicular to the direction of the wires. To further specify the model, we assume that at each position x of a given wire, the coupling strength with a neighboring wire is equal to J with

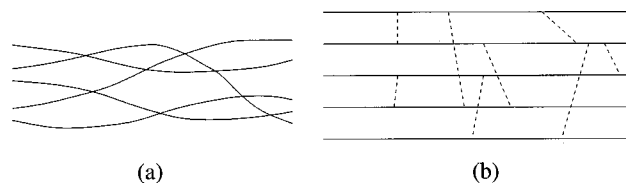


FIG. 1. (a) Schematic representation of a random network of metallic disordered wires. Each intersection between solid lines represents an interwire junction. (b) Stretching the wires, we obtain a regular lattice. The interwire junctions become interwire couplings (dashed lines).

probability c (presence of an interwire junction) and vanishes with probability $1-c$ (absence of a junction). For $M=1$, this model exactly corresponds to the one studied numerically by ZEE. It is clear that the model is meaningful only if the probability to have a junction at a given position along a wire is weak ($c \ll 1$). As pointed out in Ref. 3, the existence of a delocalized phase is a highly nontrivial phenomenon. Indeed, the random interwire coupling increases the dimensionality (which favors the delocalized phase) but is also an additional source of scattering.

We first consider the case where each fibril reduces to a single chain ($M=1$). We will show at the end of Sec. III how the results can be straightforwardly extended to an arbitrary number M of chains. The intrachain disorder is taken into account via a random potential $V_l(x)$ with zero mean and Gaussian probability distribution:

$$\langle V_l(x)V_{l'}(x') \rangle = (2\pi N_1(0)\tau)^{-1} \delta_{l,l'} \delta(x-x'), \quad (2.1)$$

where $N_1(0)$ is the density of states of the chains and τ the elastic scattering time which originates in the random potential V . The integers $l \equiv (l_1, l_2)$ refer to the positions of the chains and x to the position along the chains. In the absence of interchain coupling, the electronic states are localized with a localization length $R_0 \sim l$ where $l = v_F \tau$ is the mean free path and v_F the Fermi velocity of the 1D chains. [Notice that $N_1(0) = 1/\pi v_F$.]

The mean value of the neighboring chain coupling is $\bar{t}_\perp = cJ$. Deviations from this mean value are taken into account via a random hopping $V_{l,l'}^\perp(x)$ with second cumulant equal to

$$\begin{aligned} \langle V_{l_1, l_2}^\perp(x) V_{l'_1, l'_2}^\perp(x') \rangle &= \tilde{t}_\perp \delta(x-x') \bar{\delta}_{l_1, l_2 \pm 1} (\delta_{l_1, l'_1} \delta_{l_2, l'_2} \\ &+ \delta_{l_1, l'_2} \delta_{l_2, l'_1}), \end{aligned} \quad (2.2)$$

where $\tilde{t}_\perp = ac(1-c)J^2$. a is the lattice spacing along the chains axis. $\bar{\delta}_{l_1, l_2 \pm 1}$ means that l_1 and l_2 are first neighbors. Higher order cumulants of the random variable V^\perp are neglected, i.e., we assume that V^\perp has a Gaussian probability distribution.

In second quantized form, the Hamiltonian of the system can be written as $\mathcal{H} = \mathcal{H}_{\text{pure}} + \mathcal{H}_{\text{dis}} + \mathcal{H}_{\text{dis}}^\perp$ where (for simplicity we consider spinless fermions)

$$\begin{aligned} \mathcal{H}_{\text{pure}} &= \sum_l \int dx \hat{\psi}_l^\dagger(x) (v_F | -i\partial_x | - k_F) \hat{\psi}_l(x) \\ &\quad - \bar{t}_\perp \sum_{l, l' = l \pm 1} \int dx \hat{\psi}_l^\dagger(x) \hat{\psi}_{l'}(x), \\ \mathcal{H}_{\text{dis}} &= \sum_l \int dx V_l(x) \hat{\psi}_l^\dagger(x) \hat{\psi}_l(x), \\ \mathcal{H}_{\text{dis}}^\perp &= - \sum_{l, l'} \int dx V_{l, l'}^\perp(x) \hat{\psi}_l^\dagger(x) \hat{\psi}_{l'}(x). \end{aligned} \quad (2.3)$$

$\mathcal{H}_{\text{pure}}$ describes the 1D chains [with dispersion law $v_F(|k_x| - k_F)$ where k_F is the Fermi momentum] coupled by the transfer integral \bar{t}_\perp . \mathcal{H}_{dis} and $\mathcal{H}_{\text{dis}}^\perp$ correspond to the

intrachain disorder and the random interchain coupling, respectively. Averaging over the random potentials V and V^\perp is performed by introducing N replica of the system. Using Eqs. (2.1) and (2.2), we can write the averaged partition function of the replicated system as a functional integral over Grassmann variables $\psi^{\alpha(*)}$ ($\alpha = 1, \dots, N$):

$$Z = \int \mathcal{D}\psi^* \mathcal{D}\psi e^{-S_{\text{pure}} - S_{\text{dis}} - S_{\text{dis}}^\perp}, \quad (2.4)$$

where

$$\begin{aligned} S_{\text{pure}} &= - \sum_{\alpha, l, l'} \int dx dx' d\tau d\tau' \psi_l^{\alpha*}(x\tau) \\ &\quad \times G_{l, l'}^{-1}(x\tau, x'\tau') \psi_{l'}^\alpha(x'\tau'), \\ S_{\text{dis}} &= - \frac{(2\pi N_1(0)\tau)^{-1}}{2} \sum_{\alpha, \beta, l, l'} \int dx dx' d\tau d\tau' \psi_l^{\alpha*}(x\tau) \\ &\quad \times \psi_l^\alpha(x\tau) \psi_{l'}^{\beta*}(x\tau') \psi_{l'}^\beta(x\tau'), \\ S_{\text{dis}}^\perp &= - \frac{\tilde{t}_\perp}{2} \sum_{\alpha, \beta, l, l'} \bar{\delta}_{l, l' \pm 1} \int dx dx' d\tau d\tau' \\ &\quad \times [\psi_l^{\alpha*}(x\tau) \psi_{l'}^{\beta*}(x\tau') \psi_{l'}^\beta(x\tau') \psi_l^\alpha(x\tau) \\ &\quad - \psi_l^{\alpha*}(x\tau) \psi_{l'}^\beta(x\tau') \psi_{l'}^{\beta*}(x\tau') \psi_l^\alpha(x\tau)]. \end{aligned} \quad (2.5)$$

$\tau, \tau' \in [0, 1/T]$ are imaginary times. $G_{l, l'}^{-1}(x\tau, x'\tau')$ is the Fourier transform of $G^{-1}(\mathbf{k}, \omega_n) = i\omega_n - \epsilon(\mathbf{k})$. $\epsilon(\mathbf{k}) = v_F(|k_x| - k_F) - 2\bar{t}_\perp(\cos(k_y d) + \cos(k_z d))$ (d is the interchain spacing) and $\omega_n = \pi T(2n+1)$ (n integer) is a Matsubara frequency. As usual, the averaging over V generates an effective local (intrachain) electron-electron interaction. The averaging over V^\perp generates an effective interchain interaction. Equivalently, one can view this latter interaction as hoppings of particle-particle or particle-hole pairs between neighboring chains. For later calculations, it is convenient to express S_{dis}^\perp as a function of the Fourier transformed fields $\psi^{(*)}(\mathbf{k}\omega_n)$:

$$\begin{aligned} S_{\text{dis}}^\perp &= - \frac{1}{2LN_\perp^2} \sum_{\mathbf{k}, \mathbf{k}', \mathbf{q}} \sum_{\omega_n, \omega_m} \sum_{\alpha, \beta} \tilde{t}_\perp(\mathbf{q}_\perp) [\psi^{\alpha*}(\mathbf{k}\omega_n) \\ &\quad \times \psi^{\beta*}(\mathbf{q} - \mathbf{k}\omega_m) \psi^\beta(\mathbf{q} - \mathbf{k}'\omega_m) \psi^\alpha(\mathbf{k}'\omega_n) - \psi^{\alpha*}(\mathbf{k}\omega_n) \\ &\quad \times \psi^\beta(\mathbf{k} - \mathbf{q}\omega_m) \psi^{\beta*}(\mathbf{k}' - \mathbf{q}\omega_m) \psi^\alpha(\mathbf{k}'\omega_n)], \end{aligned} \quad (2.6)$$

where $\tilde{t}_\perp(\mathbf{q}_\perp) = 2\bar{t}_\perp(\cos(q_y d) + \cos(q_z d))$ is the Fourier transform of $\tilde{t}_\perp \bar{\delta}_{l, l' \pm 1}$. Here L is the length of the N_\perp^2 chains.

III. SELF-CONSISTENT DIAGRAMMATIC THEORY

In this section, we determine the phase diagram using the SCDT of Anderson localization.⁵ We first obtain the diffusive modes in the semiclassical approximation considering both sources of disorder (V and V^\perp) on an equal footing. From the results of Prigodin and Firsov,⁶ we then deduce the position of the MIT.

The first step is to calculate the self-energy correction in

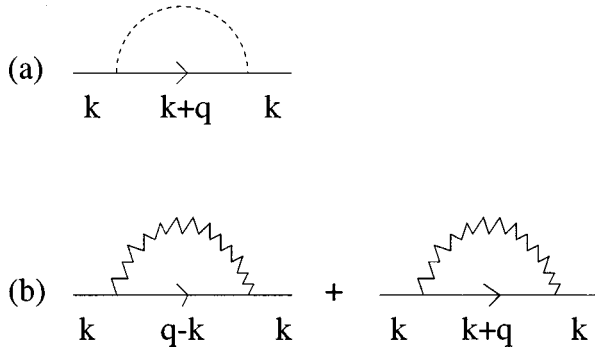


FIG. 2. Self-energy in the Born approximation. (a) Σ_1 (obtained from S_{dis}). The dashed line gives a factor $(2\pi N_1(0)\tau)^{-1}$. (b) Σ_2 (obtained from S_{dis}^\perp). The wavy line gives a factor $\tilde{t}_\perp(\mathbf{q}_\perp)$ for the first diagram and a factor $\tilde{t}_\perp(\mathbf{q}_\perp=0)$ for the second diagram (see text).

the Born approximation (Fig. 2). The contribution of the intrachain disorder V is given by

$$\Sigma_1 = \frac{(2\pi N_1(0)\tau)^{-1}}{LN_\perp^2} \sum_{\mathbf{q}} G(\mathbf{k}+\mathbf{q}, \omega_n) = -\frac{i}{2\tau} \text{sgn}(\omega_n) \quad (3.1)$$

neglecting a nonessential shift of the chemical potential and keeping only terms which do not vanish in the replica limit ($N \rightarrow 0$). In the same way, we obtain the contribution of the random potential V^\perp :

$$\Sigma_2 = \frac{1}{LN_\perp^2} \sum_{\mathbf{q}} [\tilde{t}_\perp(\mathbf{q}_\perp) G(\mathbf{q}-\mathbf{k}, \omega_n) + \tilde{t}_\perp(\mathbf{q}_\perp=0) G(\mathbf{k}+\mathbf{q}, \omega_n)]. \quad (3.2)$$

The first contribution to Σ_2 vanishes when summing over \mathbf{q} and we therefore obtain

$$\Sigma_2 = -i4\pi N_1(0) \tilde{t}_\perp \text{sgn}(\omega_n) \equiv -\frac{i}{2\tau'} \text{sgn}(\omega_n). \quad (3.3)$$

The effective transverse diffusion coefficient in Eq. (3.6) is the sum of two terms. $D_\perp'' = 8\tilde{t}_\perp^2 \tau''$ is generated by single-particle hoppings. $1/\tau' \propto \tilde{t}_\perp$ comes from particle-hole pair hopping as described by Eqs. (2.5) and (2.6).

Due to time-reversal invariance, the cooperon has the same expression as the diffuson: $\Gamma_{\text{pp}}(\mathbf{q}, \omega_\nu) = \Gamma_{\text{ph}}(\mathbf{q}, \omega_\nu)$ where the definition of the external variables \mathbf{q}, ω_ν is given by Fig. 3. $\Gamma_{\text{pp}}(\mathbf{q}, \omega_\nu)$ and $\Gamma_{\text{ph}}(\mathbf{q}, \omega_\nu)$ are characteristic of a weakly coupled chains system with Fermi velocity (along the chains) v_F , elastic scattering time τ'' , and anisotropic diffusion coefficients D'' and $D_\perp'' + 1/\tau'$. The SCDT has already

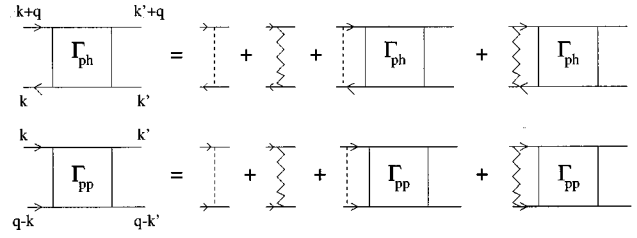


FIG. 3. Diagrammatic representation of the Bethe-Salpeter equation for the diffuson (Γ_{ph}) and the cooperon (Γ_{pp}). The wavy line represents $\tilde{t}_\perp(\mathbf{q}_\perp)$.

The total self-energy can be written as $\Sigma = -(i/2\tau'') \text{sgn}(\omega_n)$ where the scattering rate $1/\tau'' = 1/\tau + 1/\tau'$ depends on $1/\tau$ and $1/\tau' \propto c(1-c)J^2$.

The diffusive modes (diffuson and cooperon) are obtained by summing the ladder diagrams shown in Fig. 3. The diffuson is therefore given by the Bethe-Salpeter equation

$$\begin{aligned} \Gamma_{\text{ph}}(\mathbf{q}, \omega_\nu) &= [(2\pi N_1(0)\tau)^{-1} + \tilde{t}_\perp(\mathbf{q}_\perp)] \\ &\quad \times [1 + \Pi(\mathbf{q}, \omega_\nu) \Gamma_{\text{ph}}(\mathbf{q}, \omega_\nu)] \\ &= \frac{(2\pi N_1(0)\tau)^{-1} + \tilde{t}_\perp(\mathbf{q}_\perp)}{1 - [(2\pi N_1(0)\tau)^{-1} + \tilde{t}_\perp(\mathbf{q}_\perp)] \Pi(\mathbf{q}, \omega_\nu)}, \end{aligned} \quad (3.4)$$

where $\omega_\nu = \nu 2\pi T$ (ν integer) is a bosonic Matsubara frequency. We have introduced the particle-hole bubble ($\tilde{\omega}_n = \omega_n + \text{sgn}(\omega_n)/2\tau''$)

$$\begin{aligned} \Pi(\mathbf{q}, \omega_\nu) &= \frac{1}{LN_\perp^2} \sum_{\mathbf{k}} G(\mathbf{k}, \tilde{\omega}_n) G(\mathbf{k}+\mathbf{q}, \tilde{\omega}_{n+\nu}) \\ &= 2\pi N_1(0) \tau'' [1 - |\omega_\nu| \tau'' - D'' \tau'' q_x^2 \\ &\quad - D_\perp \tau'' (\sin^2(q_y d/2) + \sin^2(q_z d/2))], \end{aligned} \quad (3.5)$$

for $\omega_n \omega_{n+\nu} < 0$ and $\omega_\nu, q \rightarrow 0$. $D'' = v_F^2 \tau''$ and $D_\perp'' = 8\tilde{t}_\perp^2 \tau''$. Setting $\mathbf{q}_\perp = 0$ in the numerator of Eq. (3.4) (which is justified close to the diffusive pole), we obtain

$$\Gamma_{\text{ph}}(\mathbf{q}, \omega_\nu) = \frac{(2\pi N_1(0)\tau'')^{-1}}{|\omega_\nu| + D'' q_x^2 + (D_\perp'' + 1/\tau') (\sin^2(q_y d/2) + \sin^2(q_z d/2))}. \quad (3.6)$$

been applied to a quasi-1D system by Prigodin and Firsov.^{6,7} The position of the MIT is determined by

$$\left(D_\perp'' + \frac{1}{\tau'} \right) \tau'' = 8\tilde{t}_\perp^2 \tau''^2 + \frac{\tau''}{\tau'} = 2\gamma^2, \quad (3.7)$$

where γ is a constant of order 1. Since our final results strongly depend on the precise value of γ for $M=1$, we consider γ as an adjustable parameter. Following Refs. 3 and 4, we introduce the number of junctions per unit length $p = 4c/a$, the number of junctions within the chain localiza-

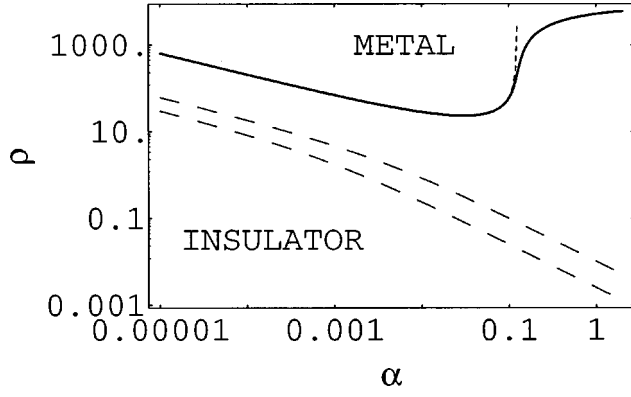


FIG. 4. Phase diagram obtained in the SCDT ($\gamma=1$). The solid line corresponds to the transition line obtained from Eq. (3.7) for $M=1$ ($t_x\tau=1000$). The dashed line corresponds to the approximation (3.9) valid for $c\ll 1$. Long-dashed lines: transition lines for $M=10$ and $M=20$.

tion length $\rho=pR_0=4cl/a$, and the dimensionless interchain coupling $\alpha=(\pi aN_1(0)J)^2$. For $c\ll 1$, we have

$$\bar{t}_\perp\tau' = \frac{1}{8(1-c)\sqrt{\alpha}} \approx \frac{1}{8\sqrt{\alpha}}, \quad \frac{\tau'}{\tau} = \frac{1}{2(1-c)\rho\alpha} \approx \frac{1}{2\rho\alpha}, \quad (3.8)$$

so that the equation which determines the position of the MIT is a function of α and ρ only:

$$\frac{1}{\rho} = 2\alpha \left(\frac{1}{4\gamma^2} - 1 \right) + \frac{\alpha}{2\gamma^2} \left(1 + \frac{\gamma^2}{\alpha} \right)^{1/2}. \quad (3.9)$$

In general, Eq. (3.7) involves α , ρ , and $t_x\tau$ where t_x is the intrachain transfer integral (since $c=\rho a/4l=\rho/8t_x\tau$).⁸ For $\gamma < 1/\sqrt{2}$, ρ is a decreasing monotonous function of α . For $\gamma > 1/\sqrt{2}$, ρ decreases for $\alpha \ll 1$ but increases when $\alpha \sim 1$. Choosing $\gamma > 1/\sqrt{2}$, we reproduce the numerical results of ZEE which show a nonmonotonous behavior of ρ as a function of α (Fig. 4). When $\alpha \ll 1$, $\tau' \gg \tau$ on the transition line. The main source of scattering comes from the intrachain disorder. The main effect of an increase of α is then to increase the effective transverse diffusion coefficient $8\bar{t}_\perp^2\tau'' + 1/\tau'$. Using $\tau/\tau' \ll 1$ and $\tau'' \sim \tau$, Eq. (3.7) reduces to $2\bar{t}_\perp\tau \sim \gamma$ which involves only $\bar{t}_\perp = cJ$ in agreement with the numerical calculation of Ref. 4. When $\alpha \sim 1$, the random interchain coupling becomes the main source of scattering ($\tau' \lesssim \tau$). This effect dominates over the increase of the effective transverse diffusion coefficient and favors the localized phase. In this regime, the position of the transition line depends on both $\bar{t}_\perp = cJ$ and $1/\tau' \propto c(1-c)J^2$. We can also obtain from Eq. (3.7) the critical intrachain disorder $W=(12t_x/\tau)^{1/2}$ as a function of J (c fixed) or c (J fixed) (Figs. 5 and 6). We obtain a very good (qualitative) agreement with the numerical calculations of ZEE (compare Figs. 5 and 6 with Ref. 4).

To conclude this section, we consider the case where the fibrils contain M 1D chains (i.e., M transverse conducting channels). At the semiclassical level, the expression of the diffusion and cooperon are unchanged and are given by Eq. (3.4). Including localization effects, we obtain a MIT determined by

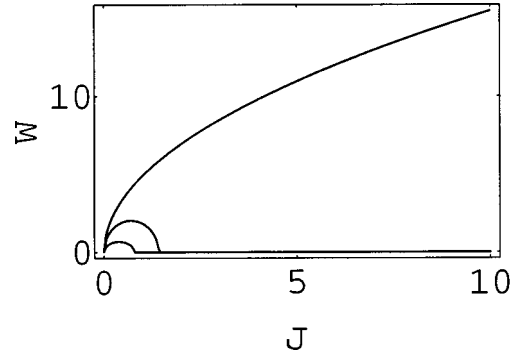


FIG. 5. Critical intrachain disorder $W=(12t_x/\tau)^{1/2}$ [$t_x=1$] in the SCDT vs J for $c=1, 0.5$, and 0.1 (from top to bottom).

$$\left(D_\perp'' + \frac{1}{\tau'} \right) \tau'' = 8\bar{t}_\perp^2 \tau''^2 + \frac{\tau''}{\tau'} = 2\frac{\gamma^2}{M^2}. \quad (3.10)$$

The dependence on M can be obtained from standard scaling arguments.⁹ In the diffusive regime, an electron diffuses to the neighboring wire within a time τ_x determined by $d^2=(D_\perp''+1/\tau')(d^2/4)\tau_x$. The corresponding diffusion length along the wire is $L_x=(D''\tau_x)^{1/2}$. The MIT in the system of coupled wires occurs when $L_x \sim R_0$ where $R_0 \sim Ml$ is the localization length of an isolated wire. This leads to Eq. (3.10).

Whatever the value of $\gamma \sim O(1)$, for $M \gg 1$ we obtain from Eq. (3.10) a monotonous decrease of ρ for increasing α in agreement with PE's results.³ However, the position of the MIT does not correspond exactly to the one obtained by PE. In particular, we find that ρ approaches zero when $\alpha \gg 1$ while PE obtained $\rho \sim 1$ in that limit. Along the transition line, the main source of scattering is always the intrachain disorder (i.e., $\tau \ll \tau'$). For $\alpha \lesssim 1$, the interchain hops are primarily due to single-particle hoppings (\bar{t}_\perp) while for $\alpha \gtrsim 1$ they are mostly due to particle-particle or particle-hole pair hoppings (\tilde{t}_\perp).

IV. NONLINEAR σ MODEL

In the preceding section, we have considered both sources of disorder (V and V^\perp) on an equal footing. We now propose a different approach where S_{dis}^\perp is treated in perturbation

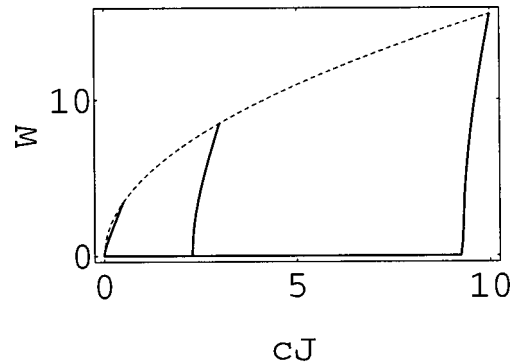


FIG. 6. Critical intrachain disorder $W=(12t_x/\tau)^{1/2}$ [$t_x=1$] in the SCDT vs cJ for various values of J ($J=0.5, 3$, and 10 from left to right). Dashed line: $W=(24t_x\bar{t}_\perp/\gamma)^{1/2}$ vs cJ .

while $S_{\text{pure}} + S_{\text{dis}}$ is treated (at least in principle) exactly. To do that, we decouple the quartic term S_{dis}^{\perp} by means of a Hubbard-Stratonovich transformation. (A similar approach has been used recently to study the MIT in quasi-2D disordered conductors.^{10,11}) We then show that the low-energy fluctuations of the auxiliary field are governed by a NL σ M from which we can deduce the position of the MIT. We consider in this section only the case $M=1$.

We introduce spinors $\phi, \bar{\phi}$ defined by

$$\phi_{ln}^{\alpha}(x) = \frac{1}{\sqrt{2}} \begin{pmatrix} \psi_l^{\alpha*}(x\omega_n) \\ \psi_l^{\alpha}(x\omega_n) \end{pmatrix},$$

$$\bar{\phi}_{ln}^{\alpha}(x) = (C\phi)^T = \frac{1}{\sqrt{2}} (-\psi_l^{\alpha}(x\omega_n), \psi_l^{\alpha*}(x\omega_n)), \quad (4.1)$$

where C is the charge conjugation operator.¹² The action S_{dis}^{\perp} is rewritten as

$$S_{\text{dis}}^{\perp}[\bar{\phi}, \phi] = \int dx \text{Tr}[B(x) \tilde{t}_{\perp} B(x)], \quad (4.2)$$

where we have introduced the matrix field $B_{lnm}^{\alpha\beta}(x) = \phi_{ln}^{\alpha}(x) \otimes \bar{\phi}_{lm}^{\beta}(x)$. In Eq. (4.2), \tilde{t}_{\perp} should be understood as the matrix $\tilde{t}_{\perp, l, l'} = \tilde{t}_{\perp} \delta_{l, l' \pm 1}$ (diagonal in the indices α, n, i where $i=1,2$ refers to the two components of the spinors). Tr denotes the trace over all discrete indices. Introducing an auxiliary matrix field $Q_{lnm}^{\alpha\beta}(x)$ to decouple Eq. (4.2), we write the partition function as

$$Z = \int \mathcal{D}\bar{\phi} \mathcal{D}\phi e^{-S_0[\bar{\phi}, \phi]} \times \int \mathcal{D}Q e^{-\int dx [\text{Tr}[Q(x) \tilde{t}_{\perp}^{-1} Q(x)] + 2i \text{Tr}[B(x) Q(x)]]}, \quad (4.3)$$

where \tilde{t}_{\perp}^{-1} is the inverse matrix of \tilde{t}_{\perp} and $S_0 = S_{\text{pure}} + S_{\text{dis}}$. (One can verify that different decouplings of S_{dis}^{\perp} would not

lead to any nontrivial phenomena.) The auxiliary field has the same structure as the field $B(x)$ and therefore satisfies the conditions $Q^+ = C^T Q^T C = Q$.¹²

We first determine the value of Q in the saddle point approximation. Assuming a solution of the form $ij(Q^{\text{SP}})_{lnm}^{\alpha\beta}(x) = Q_0 \delta_{\alpha, \beta} \delta_{n, m} \delta_{i, j}$ [$i, j=1,2$ label the four components of $Q_{lnm}^{\alpha\beta}(x)$] we obtain the saddle point equation

$$Q_0 = \frac{i}{2} \tilde{t}_{\perp}(\mathbf{q}_{\perp} = 0) \frac{1}{LN_{\perp}^2} \sum_{\mathbf{k}} G^{\text{SP}}(\mathbf{k}, \omega_n). \quad (4.4)$$

$G^{\text{SP}}(\mathbf{k}, \omega_n)$ is the single-particle Green's function calculated with the saddle point action

$$S_{\text{SP}} = S_0 + 2i \int dx \text{Tr}[B(x) Q^{\text{SP}}] = - \sum_{\alpha, \mathbf{k}, \omega_n} \psi^{\alpha*}(\mathbf{k}\omega_n) \times (i\omega_n - \epsilon(\mathbf{k}) + 2iQ_0) \psi^{\alpha}(\mathbf{k}\omega_n) + S_{\text{dis}}. \quad (4.5)$$

Taking into account S_{dis} perturbatively in the Born approximation, we obtain

$$G^{\text{SP}}(\mathbf{k}, \omega_n) = \left[i\omega_n - \epsilon_{\mathbf{k}} + \frac{i}{2\tau} \text{sgn}(\omega_n) + 2iQ_0 \right]^{-1}. \quad (4.6)$$

The saddle point equations (4.4) and (4.6) yield $Q_0 = (1/4\tau') \text{sgn}(\omega_n)$ where $1/\tau' = 8\pi N_1(0) \tilde{t}_{\perp}$ was obtained in Sec. III. Within the saddle point approximation, we therefore obtain a change of the elastic scattering time due to the random interchain hopping. The total scattering rate becomes $1/\tau'' = 1/\tau + 1/\tau'$.

We now consider the fluctuations around the saddle point solution. As in the standard localization problem,¹² the $\text{Sp}(2N)$ symmetry of the Lagrangian is spontaneously broken to $\text{Sp}(N) \times \text{Sp}(N)$. Our aim is to obtain the effective action of the (diffusive) Goldstone modes associated with this spontaneous symmetry breaking. Following Ref. 12, we shift the field according to $Q \rightarrow Q + Q^{\text{SP}} - \Omega/2$, with $ij\Omega_{lnm}^{\alpha\beta}(x) = \delta_{\alpha, \beta} \delta_{n, m} \delta_{i, j} \omega_n$, and expand the action to lowest order in Ω and Q . The partition function can be written as

$$Z = \int \mathcal{D}Q e^{-\int dx [2\text{Tr}[Q^{\text{SP}} \tilde{t}_{\perp}^{-1} Q(x)] + \text{Tr}[Q(x) \tilde{t}_{\perp}^{-1} Q(x)] - \text{Tr}[\Omega \tilde{t}_{\perp}^{-1} Q(x)]]} \langle e^{-2i \int dx \text{Tr}[Q(x) B(x)]} \rangle_{\bar{S}_0}, \quad (4.7)$$

where the average $\langle \dots \rangle_{\bar{S}_0}$ should be taken with the action

$$\bar{S}_0 = S_0 + 2i \int dx \text{Tr}[B(x) (Q^{\text{SP}} - \Omega/2)]$$

$$= - \sum_{\alpha, \mathbf{k}, \omega_n} \psi^{\alpha*}(\mathbf{k}\omega_n) (-\epsilon(\mathbf{k}) + (i/2\tau') \text{sgn}(\omega_n)) \times \psi^{\alpha}(\mathbf{k}\omega_n) + S_{\text{dis}}. \quad (4.8)$$

Performing a cumulant expansion of $\langle \dots \rangle_{\bar{S}_0}$ in Eq. (4.7) and using the stationarity conditions (4.4) and (4.6), we obtain the effective action of the Q field

$$S[Q] = \int dx \text{Tr}[Q(x) \tilde{t}_{\perp}^{-1} Q(x) - \Omega \tilde{t}_{\perp}^{-1} Q(x)]$$

$$+ 2 \int dx_1 dx_2 \langle \text{Tr}[Q(x_1) B(x_1)] \text{Tr}[Q(x_2) B(x_2)] \rangle_{\bar{S}_0}$$

$$= \int dx \text{Tr}[Q(x) \tilde{t}_{\perp}^{-1} Q(x) - \Omega \tilde{t}_{\perp}^{-1} Q(x)]$$

$$- \int dx_1 dx_2 \sum_{ji} Q_{l_1 mn}^{\beta\alpha}(x_1)_{ij} \mathcal{R}_{nm}^{\alpha\beta}(x_1 l_1, x_2 l_2)$$

$$\times ij Q_{l_2 nm}^{\alpha\beta}(x_2), \quad (4.9)$$

where a sum over repeated indices is implied. $\mathcal{R}_{nm}^{\alpha\beta}$ is defined by

$$\mathcal{R}_{nm}^{\alpha\beta}(1,2) = \begin{pmatrix} R_{nm}^{\alpha\beta}(2,1|1,2) & R_{nm}^{\alpha\beta}(2,2|1,1) \\ R_{nm}^{\alpha\beta}(1,1|2,2) & R_{nm}^{\alpha\beta}(1,2|2,1) \end{pmatrix},$$

$$\begin{aligned} R_{nm}^{\alpha\beta}(x_1 l_1, x_2 l_2 | x_3 l_3, x_4 l_4) \\ = \langle \psi_{l_1}^\alpha(x_1 \omega_n) \psi_{l_2}^\beta(x_2 \omega_m) \psi_{l_4}^{\beta*}(x_4 \omega_m) \psi_{l_3}^{\alpha*}(x_3 \omega_n) \rangle_{\bar{S}_0}. \end{aligned} \quad (4.10)$$

For a system with time reversal symmetry, the Fourier transform $\mathcal{R}_{nm}^{\alpha\beta}(\mathbf{q})$ has all its components equal to $R_{nm}^{\alpha\beta}(\mathbf{q})$. In the diffusive regime, it is easy to obtain the expression of $R_{nm}^{\alpha\beta}(\mathbf{q})$ from the action \bar{S}_0 . In the replica limit ($N \rightarrow 0$), we have for the diffusive (Goldstone) modes ($\omega_n \omega_m < 0$)

$$\begin{aligned} R_{nm}^{\alpha\alpha}(\mathbf{q})^{-1}|_{\text{diff}} \equiv \bar{R}(\mathbf{q})^{-1}|_{\text{diff}} = \frac{1}{2\pi N_1(0)} \left(\frac{1}{\tau'} + v_F^2 \tau'' q_x^2 \right. \\ \left. + 8 \bar{t}_\perp^2 \tau'' (\sin^2(q_y d/2) + \sin^2(q_z d/2)) \right). \end{aligned} \quad (4.11)$$

The saddle point Q_0 introduces a ‘‘mass’’ term in the diffusive propagator. The exact propagator $R_{nm}^{\alpha\alpha}(\mathbf{q})$ can be expressed as in (4.11) but with renormalized diffusive coefficients \bar{D}'' and \bar{D}_\perp'' replacing the bare coefficients $v_F^2 \tau''$ and $8 \bar{t}_\perp^2 \tau''$, respectively:

$$\begin{aligned} \bar{R}(\mathbf{q})^{-1} = \frac{1}{2\pi N_1(0)} \left(\frac{1}{\tau'} + \bar{D}'' q_x^2 + \bar{D}_\perp'' (\sin^2(q_y d/2) \right. \\ \left. + \sin^2(q_z d/2)) \right). \end{aligned} \quad (4.12)$$

Notice that the ‘‘mass’’ term $1/\tau'$ plays the same role as a finite frequency. $R_{nm}^{\alpha\alpha}(\mathbf{q})$ can be obtained either from \bar{S}_0 or from S_0'' but at a finite frequency $1/\tau'$. Here S_0'' is the action obtained from S_0 by the replacement $\tau \rightarrow \tau''$. Equations (4.9) and (4.12) yield

$$\begin{aligned} S[Q] = \sum_{\mathbf{q}} (\bar{t}_\perp^{-1}(\mathbf{q}_\perp) - \bar{R}(\mathbf{q})) \text{Tr}[Q(\mathbf{q})Q(-\mathbf{q})] \\ - \text{Tr}[\Omega \bar{t}_\perp^{-1} Q(\mathbf{q}=0)], \end{aligned} \quad (4.13)$$

where we have introduced the Fourier transformed field $Q(\mathbf{q})$. In Eq. (4.13) and in the following, Tr does not include a sum over the integers l (chain positions) any more. We now define a low-energy regime by the conditions $q_\perp d$, $\bar{D}'' \tau' q_x^2$, $\bar{D}_\perp'' \tau' q_\perp^2 d^2/4 \lesssim 1$ which can also be written as

$$q_x \lesssim \Lambda_x \sim (\bar{D}'' \tau')^{-1/2}, \quad q_\perp \lesssim \Lambda_\perp \sim \left(\frac{d^2}{4} + \bar{D}_\perp'' \tau' \frac{d^2}{4} \right)^{-1/2}. \quad (4.14)$$

In that regime we can expand $\bar{t}_\perp^{-1}(\mathbf{q}_\perp) - \bar{R}(\mathbf{q})$ to lowest order in \mathbf{q} . Rescaling the fields $Q \rightarrow Q/4\tau'$, we thus obtain

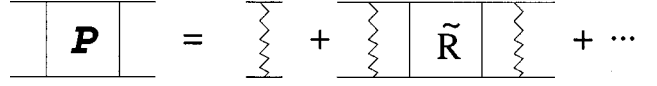


FIG. 7. Diagrammatic representation of the propagator \mathcal{P} of the Goldstone modes. The wavy line represents $\bar{t}_\perp(\mathbf{q}_\perp)$.

$$\begin{aligned} S[Q] = \frac{\pi}{8} N_1(0) \sum_{\mathbf{q}} \left(\bar{D}'' q_x^2 + \left(\bar{D}_\perp'' + \frac{1}{\tau'} \right) q_\perp^2 \frac{d^2}{4} \right) \\ \times \text{Tr}[Q(\mathbf{q})Q(-\mathbf{q})] - \frac{\pi}{2} N_1(0) \text{Tr}[\Omega Q(\mathbf{q}=0)]. \end{aligned} \quad (4.15)$$

Notice that the ‘‘mass’’ term $1/\tau'$ in the propagator $R_{nm}^{\alpha\alpha}(\mathbf{q})$ is canceled by the uniform part of $\text{Tr}[Q(x) \bar{t}_\perp^{-1} Q(x)]$ [see Eq. (4.9)]. The fluctuations of Q around its saddle point value are massless for $\omega_n \omega_m < 0$, i.e., the low-energy excitations correspond to (diffusive) Goldstone modes as expected from general symmetry arguments.¹² On the other hand, it is clear that the fluctuations are massive for $\omega_n \omega_m > 0$. Having identified the Goldstone modes, we now follow the conventional NL σ M approach. We suppress the massive fluctuations imposing on the field Q the constraints $Q^2 = \underline{1}$ (with $\underline{1}$ the unit matrix) and $\text{Tr}Q = 0$.¹² These constraints and the action (4.15) define a NL σ M.

Notice that as in the preceding section the effective transverse diffusion coefficient appearing in Eq. (4.15) is the sum of two terms. \bar{D}_\perp'' is generated by single particle interchain hopping (\bar{t}_\perp) and $1/\tau' \propto \bar{t}_\perp$ comes from particle-particle or particle-hole pair hopping as described by Eqs. (2.5) and (2.6).

Equation (4.13) shows that the propagator of the Goldstone modes is $\mathcal{P} = (\bar{t}_\perp^{-1} - \bar{R})^{-1} = \bar{t}_\perp + \bar{t}_\perp \bar{R} \bar{t}_\perp + \dots$ (see Fig. 7). Since \bar{R} is given by the exact result (4.12), it is clear that our approach does not simply consider the two sources of disorder on the same footing, but is able to take into account strong intrachain disorder effect. From this point of view, the present approach is much more satisfactory than the SCDT of the preceding section.

Going to real space and taking the continuum limit in the perpendicular directions, we eventually come to

$$\begin{aligned} S[Q] = \frac{\pi}{8} N_3(0) \int d^3 r \left[\bar{D}'' \text{Tr}[\nabla_x Q]^2 + \left(\bar{D}_\perp'' + \frac{1}{\tau'} \right) \frac{d^2}{4} \right. \\ \left. \times \text{Tr}[\nabla_\perp Q]^2 \right] - \frac{\pi}{2} N_3(0) \int d^3 r \text{Tr}[\Omega Q], \end{aligned} \quad (4.16)$$

where $N_3(0) = N_1(0)/d^2$ is the 3D density of states. The anisotropy of the diffusion coefficients being the same as that of the cutoffs (Λ_x and Λ_\perp), we can rescale the lengths according to

$$x \rightarrow x \left(\frac{\bar{D}'' \tau'}{1 + \bar{D}_\perp'' \tau' d^2} \right)^{1/3}, \quad r_\perp \rightarrow r_\perp \left(\frac{\bar{D}'' \tau'}{1 + \bar{D}_\perp'' \tau' d^2} \right)^{-1/6}, \quad (4.17)$$

in order to obtain an isotropic NL σ M:¹⁰

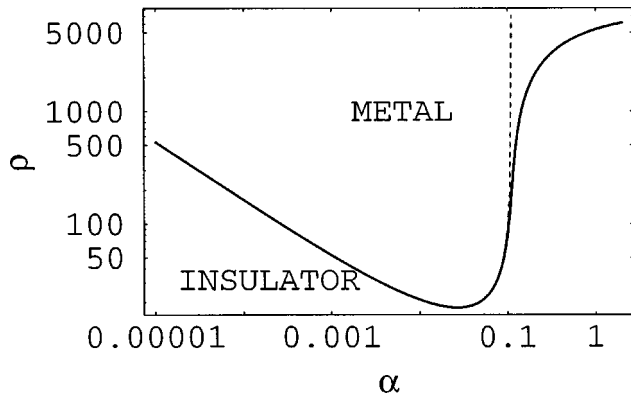


FIG. 8. Same as Fig. 4, but in the NLσM ($\gamma=1$ and $\lambda=8$).

$$S[Q] = \frac{\pi}{8} N_3(0) \bar{D} \int d^3r \text{Tr}[\nabla Q]^2 - \frac{\pi}{2} N_3(0) \int d^3r \text{Tr}[\Omega Q], \quad (4.18)$$

where

$$\bar{D} = \left[\left(\bar{D}'_{\perp} + \frac{1}{\tau'} \right) \frac{d^2}{4} \right]^{2/3} (\bar{D}'')^{1/3}. \quad (4.19)$$

The isotropic cutoff is

$$\bar{\Lambda} \sim \left(\frac{4}{(1 + \bar{D}'_{\perp} \tau') d^2} \right)^{1/3} \frac{1}{(\bar{D}'' \tau')^{1/6}}. \quad (4.20)$$

The dimensionless coupling constant of the NLσM (4.18) is

$$\lambda = \frac{4}{\pi N_3(0) \bar{D}} \bar{\Lambda} = \frac{4}{\pi N_3(0)} \frac{1}{(\mathcal{D}_{\parallel} \mathcal{D}_{\perp}^2)^{1/3} (\mathcal{D}_{\parallel} \mathcal{D}_{\perp}^2 \tau'^3)^{1/6}}, \quad (4.21)$$

where $\mathcal{D}_{\parallel} = \bar{D}''$ and $\mathcal{D}_{\perp} = (\bar{D}'_{\perp} + 1/\tau') d^2/4$ are the effective diffusion coefficients of the model before the length rescaling leading to the isotropic action (4.18). The second line of Eq. (4.21) clearly shows that the dimensionless coupling involves the geometric mean of the diffusion coefficients and the geometric mean of the diffusion lengths within a time τ' . The MIT occurs when λ equals a critical value λ_c (of order unity). To completely determine the position of the MIT, one has to obtain the diffusion coefficients \bar{D}'' and \bar{D}'_{\perp} . As mentioned above, these coefficients can be obtained from S''_0 at a finite frequency $1/\tau'$. We thus have to calculate diffusion coefficients in a weakly coupled chains system so that we can use again the results of Ref. 6. We assume that when the system is at the MIT, S''_0 corresponds to an insulating phase. We have verified that this assumption is true for $\alpha \rightarrow 0$ and $\alpha \sim 1$, and holds everywhere on the transition line if λ is sufficiently large with respect to γ . For simplicity we shall consider only the latter case by choosing $\gamma=1$ and $\lambda=8$. The MIT for S''_0 is given by $1 - 2 \bar{t}_{\perp} \tau''/\gamma = 0$ and therefore our assumption implies $1 - 2 \bar{t}_{\perp} \tau''/\gamma > 0$. The localization lengths in the insulating phase are $\xi \sim l''/|\epsilon|$ and $\xi_{\perp} \sim \xi \sqrt{2} \bar{t}_{\perp} d/v_F$ along and perpendicular to the chains, re-

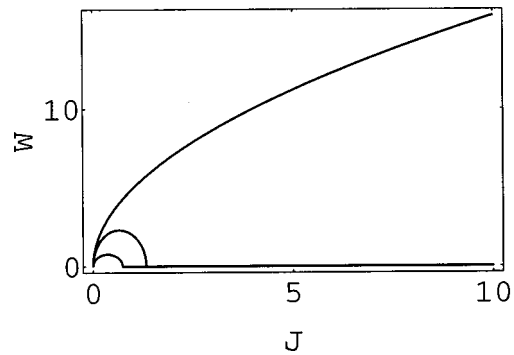


FIG. 9. Same as Fig. 5, but in the NLσM.

spectively, with $|\epsilon| = 1 - 2 \bar{t}_{\perp} \tau''/\gamma$. The finite frequency diffusion coefficients can be approximated by⁵

$$D''(\omega_{\nu}) = \frac{v_F^2 \tau''}{1 + \frac{l''^2}{\xi^2 |\omega_{\nu}| \tau''}}; \quad D'_{\perp}(\omega_{\nu}) = \frac{8 \bar{t}_{\perp}^2 \tau''}{1 + \frac{l''^2}{\xi^2 |\omega_{\nu}| \tau''}}. \quad (4.22)$$

\bar{D}'' and \bar{D}'_{\perp} are obtained from Eq. (4.22) with $|\omega_{\nu}| = 1/\tau'$. Equation (4.21) then gives the position of the MIT:

$$\left(\frac{16}{\lambda_c} \right)^2 = \frac{\tau''/\tau'}{1 + |\epsilon|^2 \tau'/\tau''} \left(1 + \frac{8 \bar{t}_{\perp}^2 \tau'' \tau'}{1 + |\epsilon|^2 \tau'/\tau''} \right)^2. \quad (4.23)$$

The preceding equation is a function of ρ , α , and $t_x \tau$. For $c \ll 1$, we can use Eq. (3.8) to obtain an equation involving only ρ and α .

Figures 8–10 show that the agreement with the SCDT is very good. The only difference is the behavior of the critical disorder W as a function of c for $c \sim 1$ (Fig. 10). We however believe this behavior to be spurious. It follows from the fact that we have mixed results from the SCDT and from the NLσM. [When $c \rightarrow 1$, $1/\tau' \rightarrow 0$ and Eq. (4.23) reduces to $|\epsilon| = 1 - 2 \bar{t}_{\perp} \tau/\gamma = 0$, i.e., $W = (24 t_x \bar{t}_{\perp} / \gamma)^{1/2}$. Thus, by using the results from Ref. 6, we impose the boundary condition $W(c=1) = (24 t_x \bar{t}_{\perp} / \gamma)^{1/2}$ which turns out not to be completely compatible with our analysis based on the NLσM.] Since the transition is described by a NLσM, we expect the critical behavior to be the usual one in agreement with the numerical calculation of ZEE,⁴ but in disagreement with PE's results.

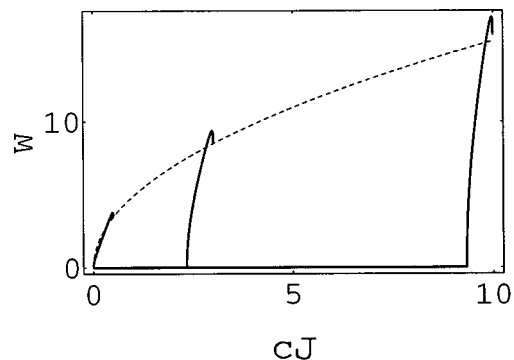


FIG. 10. Same as Fig. 6, but in the NLσM.

V. CONCLUSION

Using two different methods, we have studied the MIT in a system of randomly coupled wires. Our results clearly show the dual role of the random interwire coupling. On the one hand, it generates an effective transverse bandwidth $\bar{t}_\perp = cJ$ and gives a contribution $d^2/4\tau'$ to the transverse diffusion coefficient. On the other hand, it increases the scattering rate by $1/\tau' \propto c(1-c)J^2$. We have derived a phase diagram which agrees with the numerical calculation of ZEE (performed for $M=1$) and with the analytical analysis of PE (valid for $M \gg 1$) although we have found a different critical behavior in this latter case.

As emphasized by PE, the model studied in this paper not only yields a MIT starting from a *realistic* description of the polymer structure, but also allows one to reconcile the experimental controversy between the low- and high-temperature conductivities of polymers.³ Our zero temperature study shows that the intrafibril localization effects are suppressed by the interfibril electron hops which occur at a characteristic frequency $1/\tau' + 8\bar{t}_\perp^2\tau''$ (note that for $M \gg 1$ and $\alpha \lesssim 1$, this characteristic frequency is $\sim 1/\tau'$). At finite temperature, localization effects are also suppressed by inelastic electron-phonon collisions. Thus, at sufficiently high temperature, when $\Omega = 1/\tau' + 8\bar{t}_\perp^2\tau'' + 1/\tau_{in}(T) \gtrsim 1/\tau$ [$\tau_{in}(T)$ is the electron-phonon collision time], intrafibril lo-

calization effects are completely suppressed: the conductivity is determined by band transport and therefore increases for decreasing temperature as in a traditional metal. When $\Omega \lesssim 1/\tau$, localization effects become important. For a system close to the MIT, they lead to a decrease of the conductivity as the temperature is lowered (see Ref. 3 for a more detailed discussion).

Since $M \gg 1$ for polymers, our main conclusion agrees with PE with respect to the experimental situation in real materials: an increase of the number of interfibril contacts or the strength of the interfibril coupling should move the sample towards the metallic state. Experimentally, this is confirmed by the significant enhancement of the low-temperature conductivity under stretching or application of pressure.^{3,13,14}

ACKNOWLEDGMENTS

I am grateful to G. Montambaux and J.P. Pouget for useful discussions. I also wish to thank I. Zambetaki for sending me Ref. 4 prior to publication, C. Bourbonnais for discussions on the work reported in Ref. 11, and D. Boies for sending me a copy of his Ph.D. thesis. This work was partially supported by the NSF under Grant No. DMR-9417451 and by the David and Lucile Packard Foundation.

*On leave from Laboratoire de Physique des Solides, Université Paris-Sud, 91405 Orsay, France.

¹For a description of transport properties of highly conducting doped polymers, see contributions in *Synth. Met.* **65** (1994) and the Proceedings of the International Conference on Science and Technology of Synthetic Metals (ICSM'94) [*Synth. Met.* **69** (1994)].

²See for instance S. Kivelson and A. J. Heeger, *Synth. Met.* **22**, 371 (1988); Z. H. Wang *et al.*, *Phys. Rev. B* **43**, 4373 (1991); H. H. S. Javadi *et al.*, *ibid.* **43**, 2183 (1991); V. N. Prigodin and S. Roth, *Synth. Met.* **53**, 237 (1993).

³V. N. Prigodin and K. B. Efetov, *Phys. Rev. Lett.* **70**, 2932 (1993); *Synth. Met.* **65**, 195 (1994).

⁴I. Zambetaki, S. N. Evangelou, and E. N. Economou, *J. Phys. Condens. Matter* **8**, L605 (1996).

⁵D. Vollhardt and P. Wölfle, *Phys. Rev. B* **22**, 4666 (1980); in *Electronic Phase Transitions*, edited by W. Hanke and Yu. V. Kopayev (Elsevier, New York, 1992).

⁶V. N. Prigodin and Yu. A. Firsov, *JETP Lett.* **38**, 284 (1983); Yu. A. Firsov, in *Localization and Metal-Insulator Transition*, edited by H. Fritzsche and D. Adler (Plenum, New York, 1985).

⁷For a quasi-1D system, the results of the SCDT have been confirmed by numerical studies: O. N. Dorokhov, *Solid State Commun.* **46**, 605 (1983); **51**, 381 (1984); N. A. Panagiotides, S. N. Evangelou, and G. Theodorou, *Phys. Rev. B* **49**, 14 122 (1980).

⁸We suppose the band half-filled so that $v_F = 2at_x$.

⁹W. Apel and T. M. Rice, *J. Phys. C* **16**, L1151 (1983); N. Dupuis and G. Montambaux, *Phys. Rev. B* **46**, 9603 (1992).

¹⁰N. Dupuis (unpublished).

¹¹See also the study of the instabilities of coupled Luttinger liquids by D. Boies, C. Bourbonnais, and A.-M. S. Tremblay, *Phys.*

Rev. Lett. **74**, 968 (1995); *Correlated Fermions and Transport in Mesoscopic Systems*, Proceedings of the XXXIst Rencontres de Moriond, series: Moriond Condensed Matter Physics, France, 1996, edited by T. Martin, G. Montambaux, and J. Trân Thanh Vân (Éditions Frontières, Gif-sur-Yvette, 1996).

¹²For a review on the NL σ M approach to Anderson localization, see D. Belitz and T. R. Kirkpatrick, *Rev. Mod. Phys.* **66**, 261 (1994).

¹³A. G. McDiamird, Y. Min, J. M. Wiesinger, E. J. Oh, E. M. Scherr, and A. J. Epstein, *Synth. Met.* **55-57**, 753 (1993).

¹⁴M. Reghu, K. Vakiparta, Y. Cao, and D. Moses, *Phys. Rev. B* **49**, 16 162 (1994). These authors report that for iodine-doped (CH)_x the conductivity is found to increase a little for moderate pressure (up to 4 kbar) and decrease for greater pressure. We believe that there is no disagreement between this experimental result and the model studied in this paper or in Ref. 3. (i) Application of a moderate pressure should increase the strength of the interwire coupling and therefore the dimensionless coupling α . Clearly a moderate pressure cannot change the number of interfibril contacts (this would require a significant change of the relative positions of the fibrils and therefore a rather strong pressure) so that the parameter ρ is not changed. As shown in Fig. 4, an increase of α at fixed ρ increases the conductivity. This effect is not expected to be very large (as shown in Fig. 4, the conductivity is more sensitive to a change of ρ than of α) so that there is a rather nice agreement between theory and experiment as long as the pressure is not too strong. (ii) As reported by Reghu *et al.*, the decrease of the conductivity above 4 kbar is not fully reversible. It is very likely that this irreversibility is due to a change in the structure of the polymer (modification of the relative positions of the fibrils) which in turn induces additional defects (hence the irreversibility) and decreases the conductivity.